

# Morphology of ordering Fe-Si alloys

Y. USTINOVSHIKOV, I. SAPEGINA

*Physical-Technical Institute (Ural Branch of Russian Academy of Sciences),  
132 Kirov Street 426000, Izhevsk, Russia  
E-mail: lfp@fti.udm.ru*

The microstructure of some Fe-Si alloys water-quenched from 700–1200°C and aged at 550–675°C for various times has been studied by means of transmission electron microscopy (TEM). It has been shown that at temperatures of 700°C and above the microstructure of the alloy is a solid solution with two-dimensional particles of a B2 ordered phase. These particles have a FeSi composition and lie along (100) planes of the matrix. At temperatures of 675°C and below a modulated microstructure is formed; in its enriched modulations the composition of the Fe<sub>3</sub>Si phase is attained and D0<sub>3</sub> ordering occurs. Phase composition of some high-silicon alloys has been determined by X-ray diffraction phase analysis. It corresponds to  $\alpha + B2$  or  $\alpha + D0_3$ . These results are plotted on the accepted Fe-Si phase diagram. © 2004 Kluwer Academic Publishers

## 1. Introduction

One of the most enigmatic systems which have been studied by a great number of investigators [1–8] is the Fe-Si system in the region of a solid solution. Interpretation of some microstructural results obtained in [1–8] seems contrary to each other. This is mainly due to the fact that some systems of additional spots observed in electron diffraction patterns are difficult to identify uniquely. However, despite this fact a more or less persistent concept of the ordering processes occurring in the region of solid solutions has been formed to date; it is reflected in the presently accepted Fe-Si phase diagram [9]. According to the diagram, there are two types of the ordering of Fe and Si atoms in a solid solution. If Si concentration in an alloy is decreased or temperature is increased, the B2 ordering occurs in the bulk of the alloy. The composition of the ordered phase B2 is found to be FeSi. It is notable that with increasing Si in Fe-Si alloys the content of the silicon in an ordered phase decreases and the D0<sub>3</sub> ordering having Fe<sub>3</sub>Si composition occurs. There is also the region in the phase diagram in which the B2- and D0<sub>3</sub>-type orderings proceed simultaneously.

The results indicating the fact that the B2 ordered phase is formed at smaller silicon concentrations in the alloy in comparison with the D0<sub>3</sub> ordered phase, have been obtained by the use of X-ray diffraction, transmission electron microscopy (TEM) [1–8], neutron scattering [10] and Mössbauer spectroscopy [11, 12] methods. The difference in the intensities of the superstructural reflections in the electron diffraction patterns of Fe alloys containing 10–12.5 at.%Si is associated sometimes with the presence of a large density of antiphase boundaries in the D0<sub>3</sub> superstructure rather than with the two-phase ordering B2 + D0<sub>3</sub> [2]. The simultaneous existence of the B2 and D0<sub>3</sub> phases is considered sometimes as a result of separation of some alloys into

these phases due to the positive energy of the interaction between the nearest neighbors [13]. The system of the additional spots in the electron diffraction patterns is interpreted as relating to B2 and D0<sub>3</sub> phases simultaneously [10]. As far as neither D0<sub>3</sub> nor B2 ordering are possible in all the bulk of Fe-Si alloys containing up to 15 at.%Si, the conclusion has been made that in that Fe-Si alloys either heterogeneous short- or long-range ordering is present [13].

As is well-known, the order-disorder transitions in alloys are classified thermodynamically into two types [14], i.e., first- and second-order transitions. For second-order ones, a line at the transitional temperature  $T_0$  as a function of alloy composition separates the single-phase fields of order and disorder in the equilibrium phase diagram. Nevertheless, it is found in Fe-Si system [8] that the line for  $T_0$  terminates in a tricritical point at a composition far from stoichiometry, and below the point, the mixture of ordered and disordered phases appears in the equilibrium state. Such Fe-Si alloys are related with “tricritical systems”. Electron microscopy observations [13] have revealed that the system becomes unstable with respect to clustering as well as ordering when the composition significantly deviates from stoichiometry.

It is impossible to form perfect order at a nonstoichiometric composition. Deviation from stoichiometry degrades the degree of order attainable, leading to frustrations in a nonstoichiometric alloy if ordering tendency is significantly strong [15]. When a Fe-Si alloy is quenched into the two-phase field, the phase separation will in general follow the ordering throughout the alloy [15]. It is agreed that in the nonstoichiometric range of composition the segregation of excess atoms to antiphase boundaries and spinodal decomposition of the disordered state into two-phase mixture of ordered and disordered phases take place [16, 17].



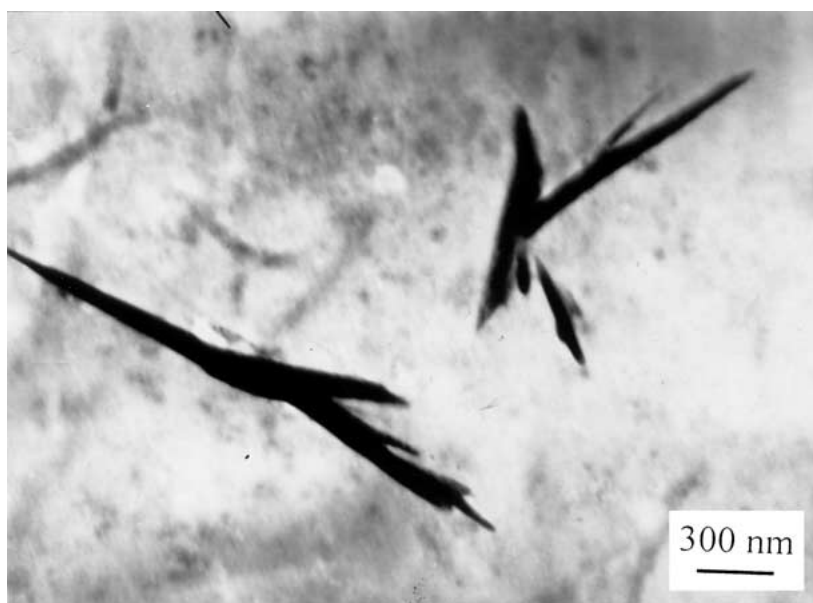
superstructure reflections a weak and uniform glowing of the entire matrix is observed but the B2 particles are not resolved. That glowing of the entire matrix is possible if the following conditions were fulfilled:

1. Particles of the B2 phase have too small sizes that they cannot be resolved by TEM.
2. Particles of the B2 phase are flat and lain only in {100} planes of a matrix.

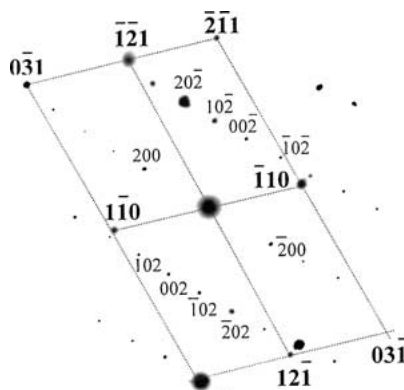
These conditions can be fulfilled if the Si atoms are arranged in the shape of monoatomic layers in the (100) planes of the matrix and separated by some layers of the Fe atoms. In this case, the Si atoms are central for the adjacent layers of the Fe atoms, i.e., they set conditions for the B2 ordering in separate matrix layers of one unit cell thickness. The electron configuration corresponding to the B2 phase forms only in the neighborhood of a monolayer of the Si atoms, i.e., here it would be expected to form a so-called two-dimensional phase. Such a “sandwich-like” ordering on the {100} planes can cause the appearance of additional spots in electron diffraction patterns. In reality, a separate particle of a two-dimensional phase cannot give any spot in

an electron diffraction pattern for reason of too small intensity of reflections from it. However, if these particles of the two-dimensional phase are formed in all the bulk of a matrix, then intensities of reflections from these particles are summed and a system of reflections from the B2 phase has been made possible to observe in an electron diffraction pattern. That system of reflections is observed at certain orientations of the foil, namely, {100} and {110}, i.e. in planes in which a density of packing of Si atoms at “sandwich-like” ordering is maximum. Now, going to the dark-field image we can see that the all matrix is weakly glowing in any additional reflection. In reality, this is due to the fact that the B2 phase particles each are glowing to give in sum that glowing which we observe in the dark-field images.

When the aging temperatures are comparatively low (550°C) and the exposure at aging temperature are from 5 to 50 h, infrequent rather large particles of irregular shape can be distinguished in the Fe-15.5 at.%Si alloy (Fig. 2a). With the aging time up to 50 h, these particles become larger. After aging of 100 h at 550°C they dissolve. When these particles emerge in the alloy microstructure, the lattice parameter of the solid solution



(a)



(b)

Figure 2 The same alloy aged at 550°C for 5 h: (a) bright-field image and (b) selected area electron diffraction pattern, orientation ratio  $(113)_\alpha \parallel (010)_{Fe_5Si_3}$ .

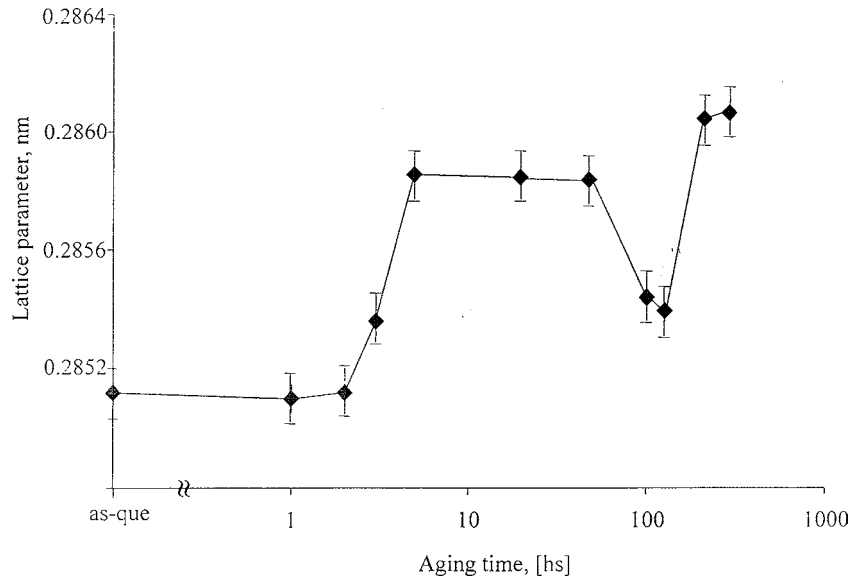
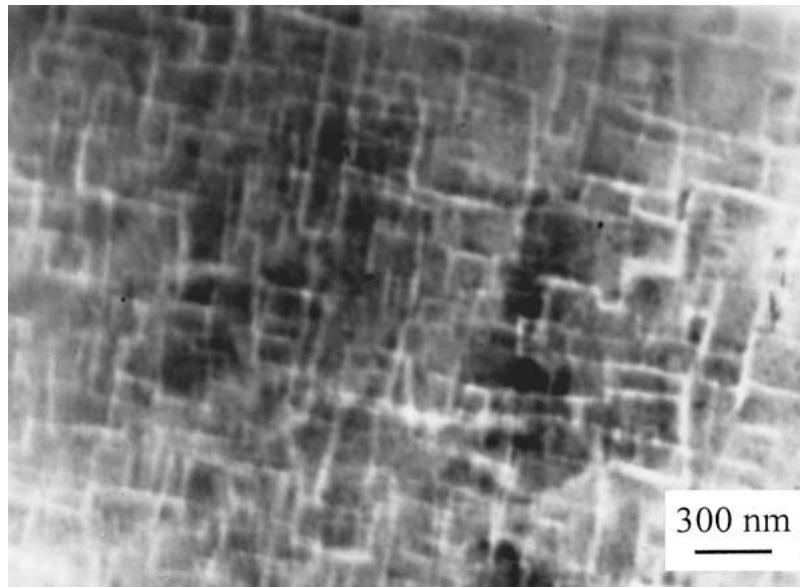


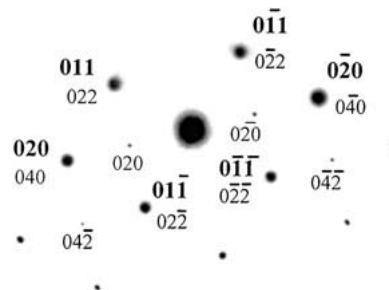
Figure 3 Lattice parameter of a solid solution versus time of aging at 550°C.

increases (Fig. 3), indicating that some Si atoms escape from the solid solution and concentrate in a phase. Interpretation of the electron diffraction pattern depicted in Fig. 2b has shown that among all the chemical compounds, which can be formed in the Fe-Si system, the only hexagonal compound  $\text{Fe}_5\text{Si}_3$  corresponds to the system of additional reflections shown in Fig. 2b. In

this case, the orientation relationship between the solid solution and the  $\text{Fe}_5\text{Si}_3$  particles is  $(113)_\alpha \parallel (010)_{\text{Fe}_5\text{Si}_3}$  (Fig. 2). The  $\text{Fe}_5\text{Si}_3$  particles are not a stable phase for the composition and temperature studied; they dissolve after 100 h of aging, which leads to the lattice parameter decrease (Fig. 3). After 200 h of aging the periodic microstructure is observed in the electron micrographs.



(a)



(b)

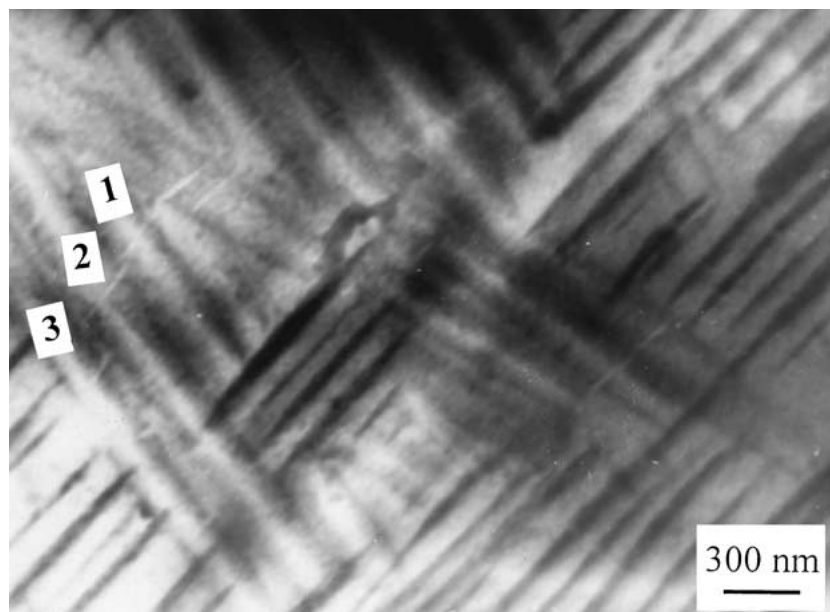
Figure 4 Fe-15.5 at.%Si alloy aged at 550°C for 200 h: (a) bright-field image, orientation of a foil is (100) and (b) selected area electron diffraction pattern.

Image of the periodic microstructure in electron micrographs strongly depends on the foil orientation. After 200 h of aging, the lattice parameter increases again (Fig. 3) indicating that once again the Si atoms participate in the formation of a phase. Fig. 4a shows the periodic microstructure which contains some light bands (the foil orientation is 100); these bands lie along  $\langle 100 \rangle$  directions of the matrix and form rectangular steps, squares and rectangles. The system of the additional reflections can be seen in the selected area electron diffraction pattern (Fig. 4b); for the case of the (100) foil orientation, the system can be interpreted as possessed by both the B2 phase and the  $D0_3$  one.

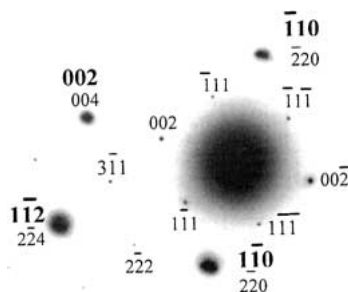
The main studies of the microstructure of the Fe 15.5 at.%Si alloy were performed after aging at  $650^\circ\text{C}$  for various times. Figs from 5 to 8 show bright-field and dark-field images of microstructures for foils of various orientations. The microstructure of the alloy after  $650^\circ\text{C}$  aging for 120 h is presented in Fig. 5 (foil orientation is 110). A typical modulated microstructure is observed in the bright-field image (Fig. 5a). An electron diffraction pattern (Fig. 5b) shows the system of the additional reflections. In order to define which (light or dark) modulations correspond to the Si-enriched solid solution (i.e., correspond to the  $D0_3$  crystal structure) the dark-field technique has been used and some light modulations in Fig. 5a have been designated by numerals 1,2,3.

Fig. 5c shows a dark-field image in the light of an additional reflection (002). Modulations marked 1,2,3 which form this reflection also are visible in Fig. 5c by the light ones. Fig. 5d demonstrates other dark-field image in the light of additional reflection ( $1\bar{1}1$ ). The same light modulations designated in Fig. 5a by numerals 1,2,3 are visible in the dark-field micrograph by the light ones (Fig. 5d). From this comparison it is obvious that the light modulations are particles enriched by Si inside of which the  $D0_3$  lattice is formed (in other words,  $D0_3$  ordering takes place). Dark modulations in the bright- and dark-field images are the portions of depleted disordered solid solution. So,  $D0_3$  ordering occurs not in all the bulk of the alloy but only in modulations enriched by Si modulations, the composition inside of which achieves a stoichiometry of the  $D0_3$  phase and  $D0_3$  lattice construct. This separation by composition with formation of enriched and depleted modulations takes place not as a result of a tendency toward separation, as expected in [10], but as a result of a tendency of nonstoichiometric compositions toward ordering (local order).

In the case of the (111) foil orientation the system of the additional spots is not observed (Fig. 6a). In the dark-field image in the light of the matrix reflection ( $1\bar{1}2$ ), the modulations are located at an angle of  $120^\circ$  relative to each other (Fig. 6b).

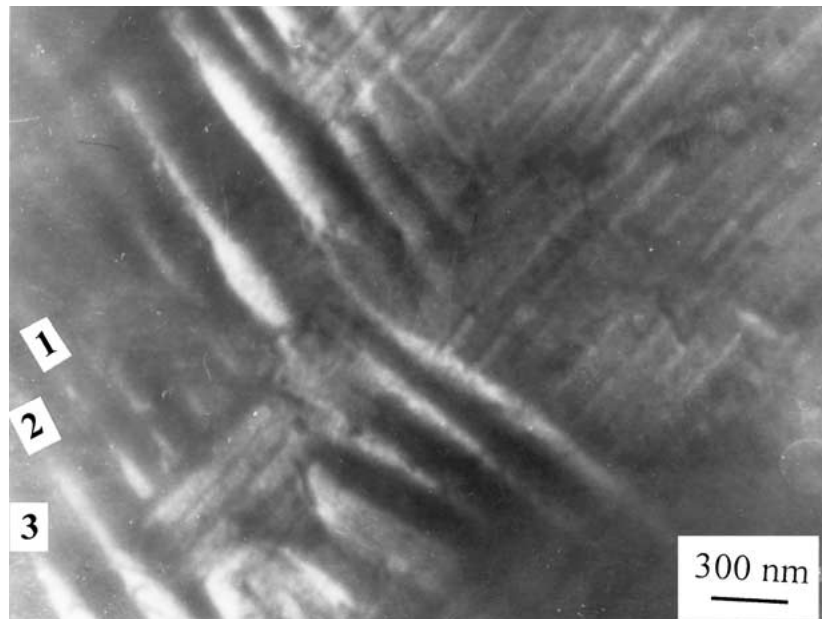


(a)

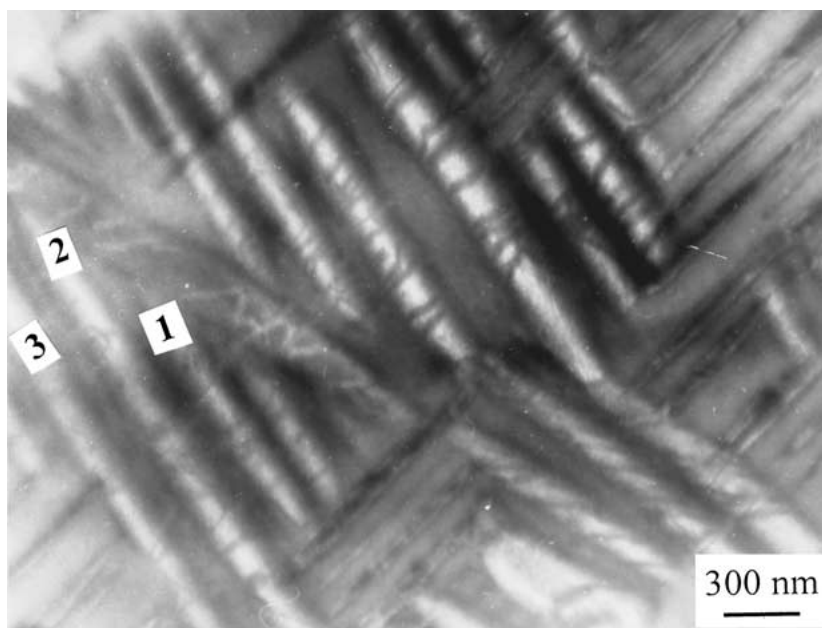


(b)

Figure 5 The same alloy aged at  $650^\circ\text{C}$  for 120 h. A foil orientation is (110): (a) bright-field image; (b) selected area electron diffraction pattern; dark-field images in the light of additional spots: (c) (002); (d) ( $1\bar{1}1$ ). (Continued.)



(c)



(d)

Figure 5 (Continued).

The bright-field image of the microstructure at the (211) orientation of a foil is shown in Fig. 7a. A typical periodic microstructure consisting of dark and light modulations, lying along  $\langle 100 \rangle$  directions of the matrix is observed. The selected area electron diffraction pattern shows a system of the additional spots (Fig. 7b), which can be interpreted as the one belonging to the  $D0_3$  structure.

Fig. 8a demonstrates an electron micrograph of the microstructure after  $650^\circ\text{C}$  aging for 120 h. The foil orientation, like in Fig. 4a, is (100). It can be seen that the microstructure is significantly coarsened in comparison with the one obtained after  $550^\circ\text{C}$  aging for 200 h. The distances between the light modulations increase almost in 2.5 times. The electron diffraction pattern in Fig. 8b is similar to the one shown in Fig. 4b. This electron diffraction pattern can be interpreted as relating

to the B2 and  $D0_3$  phases, as far as the systems of the additional spots for B2 and  $D0_3$  phases at the (100) orientation of a foil are alike. To differentiate these two types of ordering, it should be compared the electron diffraction patterns obtained at other than (100) orientations of a foil.

Comparing electron micrographs of the modulated microstructure at various orientation of the foil (Figs 4a, 5a, 6b, 7a and 8a), it is possible to appreciate spatial shape of the enriched and depleted modulations. The alloy consists of the enriched to the  $\text{Fe}_3\text{Si}$  composition rods having close to round section; the rods are parallel to  $\langle 100 \rangle$  directions of a depleted matrix.

Thus, both the B2 ordering and the  $D0_3$  ordering occur when the stoichiometry of the corresponding ordered phase is attained in local points of the alloy. For the B2 phase, these local points are layers of one unit

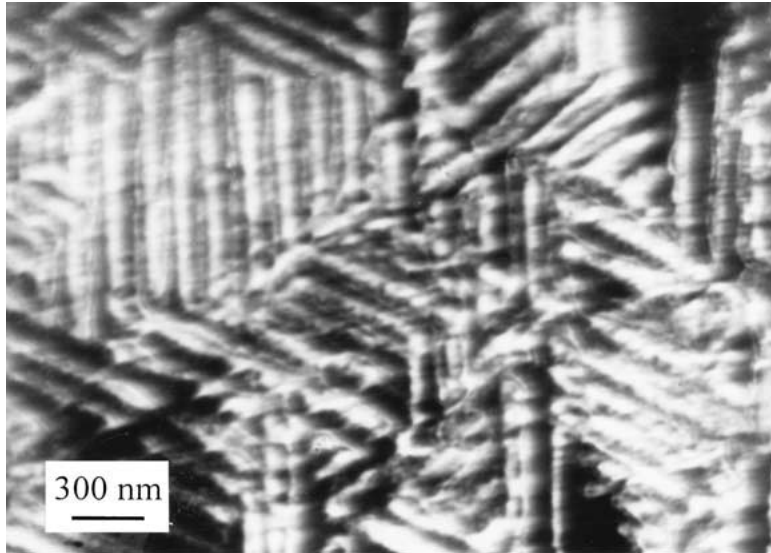
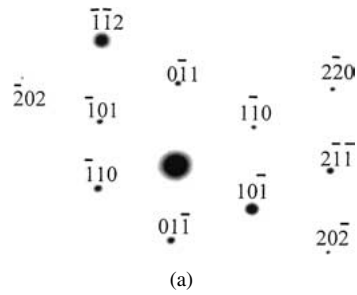


Figure 6 The same alloy aged at 650°C for 72 h. A foil orientation is (111): (a) selected area electron diffraction pattern and (b) dark-field image in the light of the matrix reflection ( $\bar{1}\bar{1}2$ ).

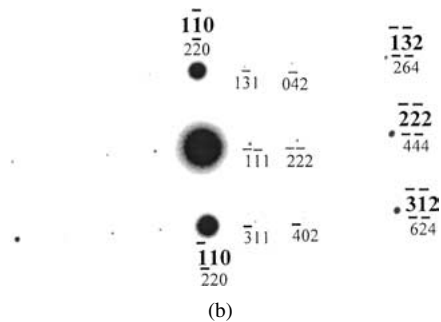
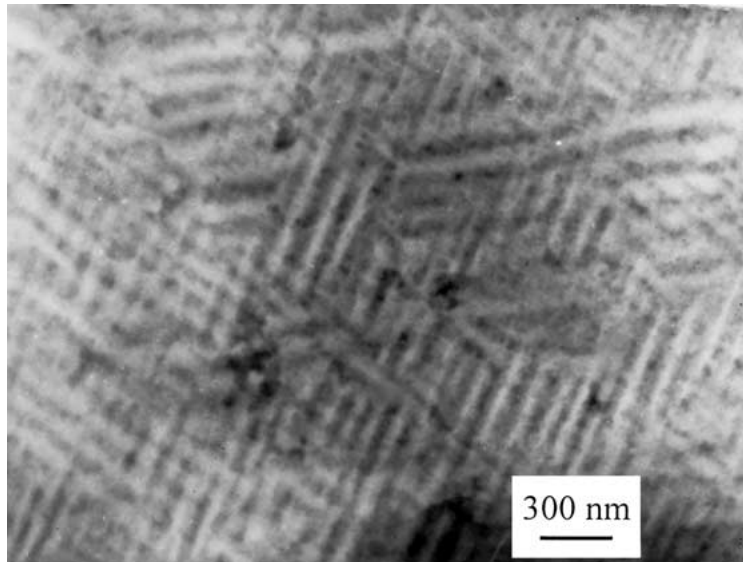
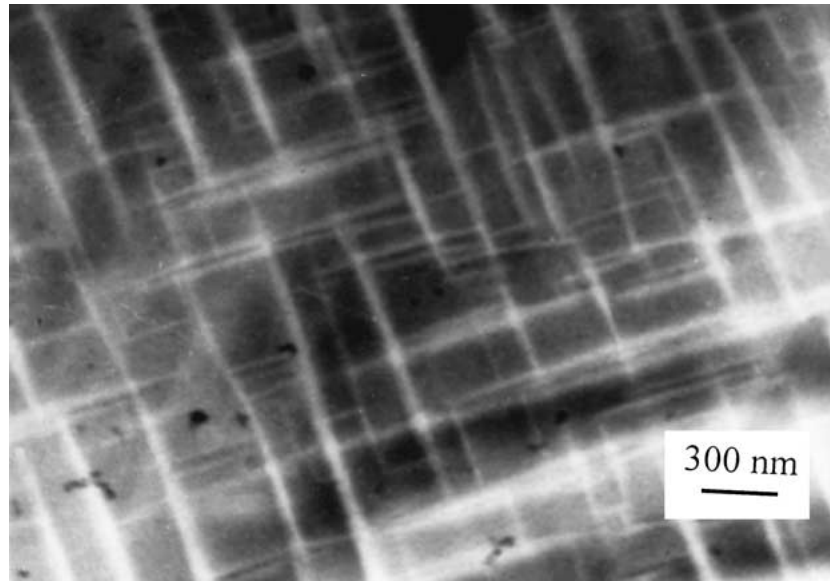
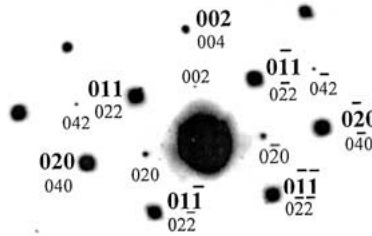


Figure 7 The same alloy aged at 650°C for 12 h. A foil orientation is (211): (a) bright-field image and (b) selected area electron diffraction pattern.



(a)



(b)

Figure 8 The same alloy aged at 650°C for 120 h. A foil orientation is (100): (a) bright-field image and (b) selected area electron diffraction pattern.

cell thickness (two-dimensional phases) lying in the {100} planes, while for the  $D0_3$  phase they are enriched in Si modulations in the shape of round rods located along  $\langle 100 \rangle$  directions of the matrix.

In order to determine the width of the region of ordering in the phase diagram on the side of less silicon concentrations, some TEM studies of the microstructure of the Fe-8.0 at.%Si alloy have been performed. The composition of the alloy lies outside the region of ordering in the Fe-Si phase diagram, though near its boundary. It has been found that the systems of the additional spots indicating one or another type of ordering are not observed in the electron diffraction patterns, i.e., microstructure of Fe-8.0 at.% Si alloy is a solid solution.

In order to determine the width of the region of ordering in the Fe-Si phase diagram on the side of higher concentrations of Si, the Fe alloys with 19 and 23 at.%Si have been studied. Because brittleness of the alloys with that Si content does not allow the production of foils for the TEM by the conventional methods, the studies employed the X-ray phase analysis. A wavelength of modulations for the case of the  $D0_3$  phase formation and thickness of layers of the B2 phase in the alloy Fe-15.5%Si are rather smaller than an area of the coherent scattering of the X-rays, therefore, the lines from the  $D0_3$  and B2 phases are absent in the X-ray diffraction patterns of this alloy. With the increase of the Si content, the above-mentioned microstructures considerably coarsen; so, it becomes possible to observe the lines from these phases in the X-ray diffraction pat-

terns obtained for Fe alloys contained 19 and 23 at.% Si. Fig. 9 shows the X-ray diffraction patterns of these alloys: besides the lines of a solid solution the superstructure lines (111), (200) and (311) are observed for the Fe-23% Si alloy (Fig. 9a), and the superstructure line (200) is observed for the Fe-19% Si one (Fig. 9b). Appearance of  $D0_3$  lines in the X-ray diffraction patterns of the Fe-23 at.%Si alloy is explained by the fact that the composition of the alloy is very close to stoichiometric one ( $Fe_3Si$ ), and, therefore, about 90% of the bulk of this alloy may be able to transform into  $D0_3$  phase. However, the intensity of the X-ray lines of  $D0_3$  phase are of significantly lower intensity than the A2 phase lines (Fig. 9) indicating that ordering touches on a small part of the bulk of the alloy. It is quite possible that the high elastic stresses attending with the  $A2 \rightarrow D0_3$  transformation are responsible for a small fraction of the bulk undergone to ordering.

Fe-19 at.% Si alloy as-quenched from 1200°C in water gives the B2 lines in the X-ray diffraction pattern; the intensities of these lines are well below the intensity of the  $D0_3$  lines (Fig. 9). The latter fact signifies that: (a) sizes of the particles of B2 phase in the Fe-19 at.%Si alloy are more than areas of the coherent scattering of the X-rays; (b) the B2 phase particles occupy only insignificant part of the bulk of the alloy, and therefore, the B2 region in the Fe-Si phase diagram is two-phase one—A2 + B2.

Results of our TEM and X-ray diffraction studies on ordering Fe-Si alloys allow a conclusion that the



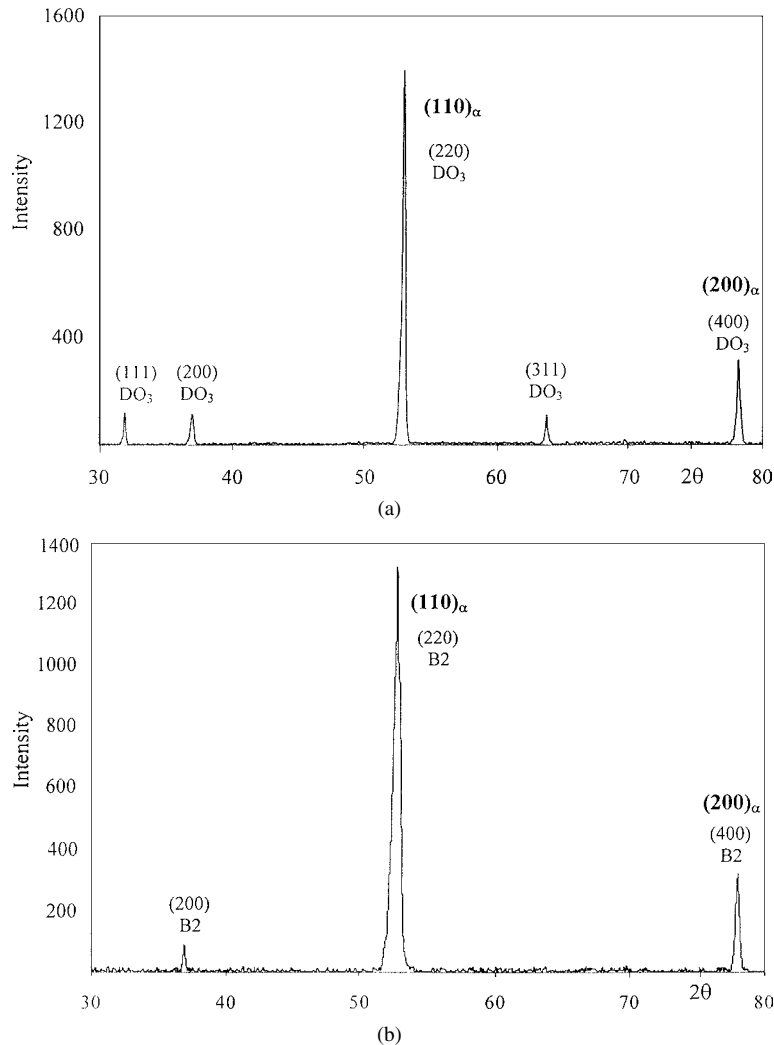


Figure 9 Fe-23 at.%Si (a) and Fe-19 at.%Si (b) alloys heated at 1200°C for 1 h prior to water-quenching. X-ray diffraction patterns.

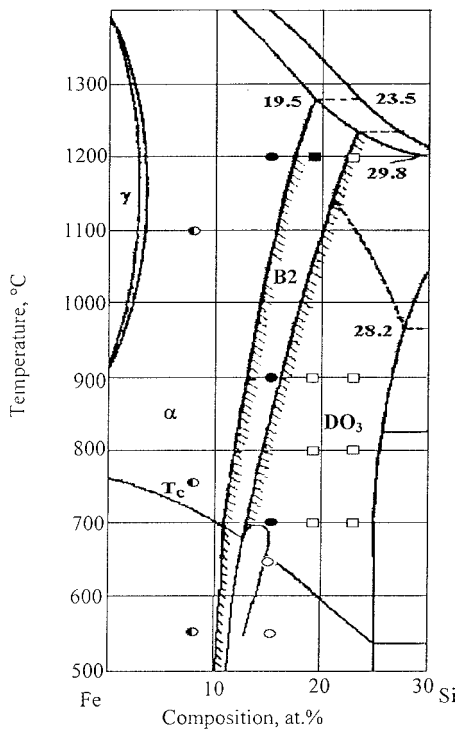


Figure 10 Fe-rich portion of the Fe-Si phase diagram. Designations are used:  $\circ$ :  $\alpha + \text{DO}_3$  on TEM data,  $\bullet$ :  $\alpha + \text{B2}$  on TEM data,  $\circ$ : a solid solution on TEM data,  $\square$ :  $\alpha + \text{DO}_3$  on X-ray diffraction data, and  $\blacksquare$ :  $\alpha + \text{B2}$  on X-ray diffraction data.

accepted Fe-Si phase diagram in the region of solid solutions does not correspond to actual relationship between the different regions ordering and does not correspond to phase composition of these regions of ordering. We have plotted our structural results on the accepted Fe-Si phase diagram (Fig. 10). According to these data, the mono-phase regions of B2 or  $\text{DO}_3$  ordering are not found; ordering process touches only small part of the bulk of a solid solution and, therefore, regions of ordering are two-phase ones:  $\text{A2} + \text{B2}$  or  $\text{A2} + \text{DO}_3$ . In this case the region of joint existence of B2 and  $\text{DO}_3$  ordering in the accepted Fe-Si phase diagram is also bound to contain an A2 solid solution resulting in violating the phase rule of Gibbs. Therefore, the  $\text{B2} + \text{DO}_3$  region in a Fe-Si phase diagram cannot exist in reality.

#### 4. Conclusion

Based on the experimental results the following conclusions can be made:

1. The B2 ordering occurs at temperatures of 700°C and above and it appears in the formation of the B2 phase layers of one unit cell thickness, lying parallel to the {100} planes of the matrix; they are separated by several layers of the Fe atoms. Such “sandwich-like” B2 ordering results in the formation of the system of the additional spots at the (100) and (110) foil orientations.

2. Prior to the  $D0_3$  ordering the formation of the Si enriched and Si depleted clusters in the form of a modulated microstructure has taken place. In the enriched modulations, the  $Fe_3Si$  stoichiometric composition is attained with time of heat treatment, and the  $D0_3$  lattice is formed.

3. The B2 ordering as well as the  $D0_3$  ordering occur in their own regions of the phase diagram due to the heterogenization of the solid solution and attainment of the stoichiometric composition in the enriched clusters ( $D0_3$ ) or in the layers of an unit cell thickness (B2). These two types of ordering cannot proceed simultaneously in the alloy, therefore, there are no the B2 +  $D0_3$  region in the Fe-Si phase diagram and the tricritical point into the miscibility gap.

4. The B2  $\rightarrow$   $D0_3$  phase transition goes through metastable  $Fe_5Si_3$  phase formation.

## References

1. W. PEPPERHOLF and H. ETTWIG, *Arch. Eisenhüttenw.* **39** (1968) 307.
2. F. GEMPERLE, *Trans. Met. Soc. AIME* **242** (1968) 2287.
3. H. WARLIMONT, *Z. Metallkunde* **59** (1968) 595.
4. G. INDEN, *ibid.* **66** (1975) 577.
5. G. INDEN and W. PITSCH, *ibid.* **62** (1971) 627.
6. G. INDEN, *ibid.* **68** (1977) 529.
7. H. ETTWIG and W. PEPPERHOFF, *ibid.* **63** (1972) 453.
8. P. R. SWANN, L. GRANAS and B. LEHTINEN, *Met. Sci.* **9** (1975) 90.
9. O. KUBASCHEWSKI, "Phase Diagrams of Binary Fe-based Systems" (Springer Verlag, Berlin-Heidelberg and Verlag Stahleisen GmbH, Dusseldorf, 1982) p. 135.
10. K. HILFRICH, W. KOLKER, W. PETRY, O. SCHARPF and E. NEMBACH, *Acta Metall. Mater.* **42** (1994) 743.
11. G. RIXECKER, P. SCHAFF and U. GONSER, *Phys. Stat. Sol. (a)* **139** (1993) 309; **151** (1995) 291.
12. O. SCHNEEWEISS, *J. Phys.: Condens. Mat.* **1** (1989) 4749.
13. T. MIYAZAKI, T. KOZAKAI and T. TSUZUKI, *J. Mater. Sci.* **21** (1986) 2557.
14. D. DE FONTAINE, "Solid State Physics," Vol. 34 (Academic Press, N.-Y., 1979) p. 73.
15. S. MATSUMURA, *Z. Metallkunde* **89** (1998) 814.
16. S. MATSUMURA, H. OYAMA and K. OKI, *Mater. Trans. JIM* **30** (1989) 695.
17. L. POSCHMANN, C.-G. OERTEL, J. BERGMANN and J. TOBISCH, *Phil. Mag. A* **71** (1995) 1083.
18. Y. P. JEANNIN, "Problems of Nonstoichiometry" (North-Holland Publishing Company, Amsterdam-London, 1970) p. 97.

Received 23 July 2002  
and accepted 4 September 2003